Mon. Not. R. Astron. Soc. **000**, 1–8 (2007) Printed 2 September 2008 (MN LATEX style file v2.2)

Thermal disc emission from a rotating black hole: X-ray polarization signatures

M. Dovčiak,[1⋆] F. Muleri,[2,3] R. W. Goosmann,[1] V. Karas[1] and G. Matt[4]

[1] *Astronomical Institute, Academy of Sciences of the Czech Republic, Boční II 1401a, CZ-141 31 Prague, Czech Republic*
[2] *Istituto di Astrofisica Spaziale e Fisica Cosmica, Via del Fosso del Cavaliere 100, I-00133 Roma, Italy*
[3] *Università di Roma Tor Vergata, Dipartimento di Fisica, via della Ricerca Scientifica 1, I-00133 Roma, Italy*
[4] *Dipartimento di Fisica, Università degli Studi "Roma Tre", Via della Vasca Navale 84, I-00146 Roma, Italy*

Accepted .... Received ...

ABSTRACT

Thermal emission from the accretion disc around a black hole can be polarized, due to Thomson scattering in a disc atmosphere. In Newtonian space, the polarization angle must be either parallel or perpendicular to the projection of the disc axis on the sky. As first pointed out by Stark and Connors in 1977, General Relativity effects strongly modify the polarization properties of the thermal radiation as observed at infinity. Among these effects, the rotation of the polarization angle with energy is particularly useful as a diagnostic tool.

In this paper, we extend the Stark and Connors calculations by including the spectral hardening factor, several values of the optical depth of the scattering atmosphere and rendering the results to the expected performances of planned X-ray polarimeters. In particular, to assess the perspectives for the next generation of X-ray polarimeters, we consider the expected sensitivity of the detectors onboard the planned POLARIX and IXO missions. We assume the two cases of a Schwarzschild and an extreme Kerr black hole with a standard thin disc and a scattering atmosphere. We compute the expected polarization degree and the angle as functions of the energy as they could be measured for different inclinations of the observer, optical thickness of the atmosphere and different values of the black hole spin. We assume the thermal emission dominates the X-ray band. Using the flux level of the microquasar GRS 1915+105 in the thermal state, we calculate the observed polarization.

Key words: polarization – relativity – X-rays: binaries – instrumentation: polarimeters

1 INTRODUCTION

The imprints of General Relativity (GR) effects on the radiation emitted in the inner regions of the accretion disc around the black hole in Active Galactic Nuclei (AGN) and Galactic black hole systems (GBHS) have been the subject of intense observational efforts in the recent past. The iron line spectroscopy has been so far the most used and successful technique to study GR effects and to estimate the black hole spin in both classes of objects (see Miller 2007 for a recent review and references therein). Recently, continuum measurements have also been shown to be a promising technique for GBHS (e.g. Liu et al. 2008).

X-ray polarimetry is also a potentially very powerful technique in this respect, as shown by Matt (1993) and Dovčiak, Karas & Matt (2004a) for AGN. For GBHS, Stark & Connors (1977); Connors & Stark (1977) and Connors, Stark & Piran (1980) discussed the GR effects on the polarization properties of the thermal emission of the accretion disc. They showed that a strong variation of the polarization angle and degree with energy, due to the radial dependence of the temperature, is induced. In this paper we reconsider and extend the Stark and Connors calculations, mainly we consider the scattering atmosphere with different optical depths.

We assume the Kerr metric for the gravitational field, a standard thin disc with a scattering atmosphere for the accretion flow and Thomson scattering in the disc atmosphere as the origin of polarization. The resulting polarization angle and degree will be shown as functions of the energy for different inclinations of the observer, optical thickness of the atmosphere and black hole spins.

⋆ E-mail: dovciak@astro.cas.cz

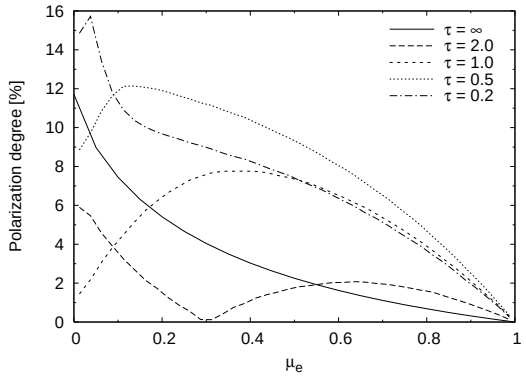

Figure 1. The dependence of the local polarization degree on the cosine of the emission angle. Curves for different optical depths τ are shown. The results for $\tau \gtrsim 5$ do not differ much from the case $\tau = \infty$.

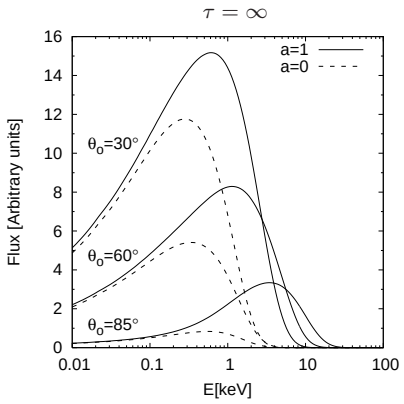

Figure 2. The multicolour black body spectra (energy flux $f_{\rm o}E$) for the extreme Kerr (solid line) and Schwarzschild (dashed line) black hole for the three observer inclinations of 30°, 60° and 85° and for the semi-infinite atmosphere.

The advent of a new generation of X-ray polarimeters (Costa et al. 2001) makes the observation of the effects discussed in this paper feasible. We will discuss the observational perspectives for a bright GBHS, the well-known high inclination microquasar GRS 1915+105, for both a relatively small polarimetric mission like POLARIX (Costa et al. 2006) and for the polarimeter aboard IXO (Bellazzini et al. 2006b).

2 ASSUMPTIONS OF THE MODEL

We assume a Keplerian, geometrically thin and optically thick disc around a black hole (Shakura & Syunyaev 1973). A full General Relativity treatment is adopted (Page & Thorne 1974). We will show results for both a Schwarzschild ($a = 0$) and an extreme Kerr ($a = 1$) black hole, where a is the dimensionless angular momentum per unit mass of the black hole. At each radius the disc is assumed to emit as a black body, modified by Thomson scattering (see below). The radial dependence of the temperature is given by the Novikov-Thorne relativistic expression to which we add the hardening factor $f_{\rm col}$ correction,

$$T(r,a) \approx 741\, f_{\rm col} \left[\frac{\dot{M}}{M_\odot/y}\right]^{1/4} \left[\frac{M_\bullet}{M_\odot}\right]^{-1/2} R(r,a) \qquad (1)$$

where $R(r,a) = r^{-3/4}\,[\mathcal{L}(r,a)/\mathcal{C}(r,a)]^{1/4}$ and $\mathcal{L}(r,a)$ and $\mathcal{C}(r,a)$ are functions of the radius and black hole spin (see Novikov & Thorne 1973 for the details). We suppose that there is zero torque at the inner edge of the disc, which is assumed to be coincident with the innermost stable circular orbit, i.e., $r_{\rm ISCO} = 6\,r_{\rm g}$ (for Schwarzschild black hole) and $r_{\rm ISCO} = 1\,r_{\rm g}$ (for an extreme Kerr black hole) with $r_{\rm g} = GM/c^2$.

We also assume that photons are scattered in the atmosphere of the disc and thus the observed radiation is polarized. We assume Thomson scattering and no absorption in the atmosphere. The resulting polarization in the local reference frame of the disc atmosphere is computed using the Monte Carlo code STOKES (Goosmann & Gaskell 2007) for finite optical depths; for infinite optical depths we adopt Chandrasekhar's analytical formula (Chandrasekhar 1960). In Fig. 1, the polarization degree we obtain for the local disc emission is plotted versus the cosine of the emission angle, μ_e, and for different vertical optical Thomson depths, τ, of the scattering atmosphere. For $\tau \lesssim 1$ the polarization vector of the emission is aligned with the projected symmetry axis of the accretion disc. At higher optical depths, the direction of the polarization vector switches to a perpendicular one with respect to the symmetry axis. The intermediate case with $\tau = 2$ has parallel polarization for $\mu_e > 0.3$ and perpendicular polarization otherwise.

The effect of hardening of the energy of photons due to scattering is modelled by a hardening factor, which increases the effective temperature (Shimura & Takahara 1995). In Fig. 2 we show the multicolour black-body energy flux integrated over the whole disc as it would be measured by a distant observer. The normalization of the flux scales with the cosine of the inclination angle. For the extreme Kerr black hole, the disc can extend closer to the black hole horizon and therefore reach higher temperatures. Therefore, the emission is stronger and harder in this case. Here, and in all computations we assume the mass of the central black hole $M_\bullet = 14 M_\odot$, the accretion rate $\dot{M} = 1.4 \times 10^{18}$ g/s and the hardening factor $f = 1.7$. With this choice, the maximum temperature in the disc is 0.389 keV at the radius $10\,r_{\rm g}$ in the Schwarzschild case and 1.985 keV at $1\,r_{\rm g}$ in the extreme Kerr case.

The assumption of a pure scattering atmosphere is the most critical one as far as the polarization is concerned. If the absorption opacity of the atmosphere is not negligible, the polarization degree is reduced and the polarization angle, for large optical depths, can even switch from perpendicular (as for a pure scattering atmosphere) to parallel to the projection of the axis on the sky (e.g. Laor, Netzer & Piran 1990; Matt, Fabian & Ross 1993). Our assumption is therefore optimistic; a more realistic calculation would need a detailed modelling of the disc atmosphere. We stress here that, whatever the absorption opacity is, in the Newtonian case (i.e. when the effects of special and general relativity are neglected) the polarization, for symmetry reasons, must be either parallel or perpendicular to the projection of the disc axis onto the sky. The continuous variation of the po-

larization angle with energy (see the next section) is a clear signature of the GR effects.

Once the photons leave the atmosphere the polarization vector can be rotated due to the strong gravity of the central black hole. The emission is amplified by the transfer function (Cunningham 1975; Dovčiak, Karas & Yaqoob 2004b) and the energy of photons is shifted by the gravitational and Doppler effects.

We assume that scattering occurs in a non-expanding atmosphere, so we use the transfer function computed for the equatorial plane and we do not include the additional rotation of the polarization angle that could be caused by the bulk outflow velocity (see Beloborodov 1998).

Also one can expect that magnetic fields of the disc atmosphere (Silantev & Gnedin 2008) will interfere the observed polarization. However, the energy-resolved dependency of the thermal component exhibits a rather unique profile which distinguishes the gravitational effects from other influences.

As the most promising polarimeters presently designed work in X-rays above a few keV, in this paper we limit ourselves to investigate the case of a stellar mass black hole (for AGN, the thermal emission is dominant in the UV band).

3 NUMERICAL IMPLEMENTATION

The main current application of our code is within the XSPEC data-fitting package, however, its applicability goes beyond that: the code can be compiled in a stand-alone mode, capable of examining polarimetrical quantities in the strong-gravity regime (see Dovčiak 2004; Dovčiak et al. 2004b; 2004c).

Properties of radiation are described in terms of photon numbers. For a point-like source, the measured flux in the solid angle $\mathrm{d}\Omega_\mathrm{o}$ is associated with the detector area $\mathrm{d}S_\mathrm{o}{\equiv}D^2\,\mathrm{d}\Omega_\mathrm{o}$. This relation defines the distance D between the observer and the source. The observed photon flux per unit solid angle in the energy bin $\langle E, E+\Delta E\rangle$, $\Delta f_\mathrm{o} \equiv \mathrm{d}N/\mathrm{d}t\,\mathrm{d}\Omega_\mathrm{o}$, is

$$\Delta f_\mathrm{o} = \int_{r_\mathrm{in}}^{r_\mathrm{out}} \mathrm{d}r\, r \int_{\phi}^{\phi+\Delta\phi} \mathrm{d}\varphi \int_{E/g}^{(E+\Delta E)/g} \mathrm{d}E_\mathrm{l}\, f_\mathrm{l}\, G, \qquad (2)$$

where $G \equiv g^2 l \mu_\mathrm{e}$ is the transfer function with g, l and μ_e being the energy shift, lensing and cosine of the emission angle, respectively, and

$$f_\mathrm{l} \equiv \frac{\mathrm{d}N_\mathrm{l}}{\mathrm{d}\tau\,\mathrm{d}S_\mathrm{l}\,\mathrm{d}\Omega_\mathrm{l}\,\mathrm{d}E_\mathrm{l}} \qquad (3)$$

is a local photon flux emitted from the surface of the disc. For a derivation of the equation (2) and a more detailed description of numerical computations of the transfer function see Dovčiak (2004) and Dovčiak et al. (2004c).

Let us define the specific Stokes parameters,

$$i_\nu \equiv \frac{I_\nu}{E}\,, \quad q_\nu \equiv \frac{Q_\nu}{E}\,, \quad u_\nu \equiv \frac{U_\nu}{E}\,, \quad v_\nu \equiv \frac{V_\nu}{E}\,, \qquad (4)$$

where I_ν, Q_ν, U_ν and V_ν are Stokes parameters for light with frequency ν (further on, we drop the index ν but we will always consider these quantities for light of a given frequency).

The integrated specific Stokes parameters (per energy bin $\langle E, E+\Delta E\rangle$), i.e. Δi_o, Δq_o, Δu_o and Δv_o are the quantities that the observer determines from the local specific Stokes parameters i_l, q_l, u_l and v_l on the disc in the following way:

$$\Delta i_\mathrm{o} = \int \mathrm{d}S \int \mathrm{d}E_\mathrm{l}\, i_\mathrm{l}\, G\,, \qquad (5)$$

$$\Delta q_\mathrm{o} = \int \mathrm{d}S \int \mathrm{d}E_\mathrm{l}\, [q_\mathrm{l}\cos 2\Psi - u_\mathrm{l}\sin 2\Psi]\, G\,, \qquad (6)$$

$$\Delta u_\mathrm{o} = \int \mathrm{d}S \int \mathrm{d}E_\mathrm{l}\, [q_\mathrm{l}\sin 2\Psi + u_\mathrm{l}\cos 2\Psi]\, G\,, \qquad (7)$$

$$\Delta v_\mathrm{o} = \int \mathrm{d}S \int \mathrm{d}E_\mathrm{l}\, v_\mathrm{l}\, G\,. \qquad (8)$$

Here, $\mathrm{d}S = r\,\mathrm{d}r\,\mathrm{d}\varphi$ is the integration element of the coordinate area on the disc and Ψ is a change of the polarization angle. The integration boundaries are the same as in eq. (2). As can be seen from the definition, the first specific Stokes parameter is equal to the photon flux, therefore, eqs. (2) and (5) are identical.

In eqs. (5)–(8) we used a law of transformation of the Stokes parameters by the rotation of axes, see eqs. (I.185) and (I.186) in Chandrasekhar (1960).

An alternative customary way of expressing polarization is in terms of degree of polarization P_o and two polarization angles χ_o and ξ_o, defined by $P_\mathrm{o} = \sqrt{q_\mathrm{o}^2+u_\mathrm{o}^2+v_\mathrm{o}^2}/i_\mathrm{o}$, $\tan 2\chi_\mathrm{o} = u_\mathrm{o}/q_\mathrm{o}$, and $\sin 2\xi_\mathrm{o} = v_\mathrm{o}/\sqrt{q_\mathrm{o}^2+u_\mathrm{o}^2+v_\mathrm{o}^2}$. However, these relations can be used only when we are interested in energy dependence of polarization. If we want to compute the polarization in certain broad energy range we need to integrate the Stokes parameters and use them instead of the specific Stokes parameters to get the correct result.

Various physical effects can influence polarization of light as it propagates towards an observer. Here we examine only the influence of the gravitational field represented by the vacuum Kerr space-time. The change of the polarization angle Ψ is defined as the angle by which a vector parallelly transported along the light geodesic rotates with respect to some chosen frame. We define it in this way because in vacuum the polarization vector is parallelly transported along the light geodesic. This angle depends on the choice of the local frame at the disc and at infinity. At the disc we consider the local frame co-moving with it with the x-axis in the direction $-\partial/\partial\theta$ in the plane defined by the normal of the disc n^μ and the momentum p_e^μ of the emitted photon. It is perpendicular to the momentum p_e^μ. The y axis lies in the plane of the disc, is perpendicular to the momentum p_e^μ and has direction $-\partial/\partial\varphi$. At infinity we consider static frame attached to the observer's sky with x-axis identified with the impact parameter β (defined as positive in the direction $-\partial/\partial\theta$) and y-axis identified with the impact parameter $-\alpha$ (α is defined as positive in the direction $\partial/\partial\varphi$).

The change of polarization angle Ψ is (see Connors et al. 1980)

$$\tan\Psi = \frac{Y}{X}\,, \qquad (9)$$

where

$$X = -(\alpha - a\sin\theta_\mathrm{o})\kappa_1 - \beta\kappa_2\,, \qquad (10)$$

$$Y = (\alpha - a\sin\theta_\mathrm{o})\kappa_2 - \beta\kappa_1\,, \qquad (11)$$

with the black hole spin a positive when the black hole rotates counter-clockwise, i.e. in the direction $\partial/\partial\varphi$. The angle

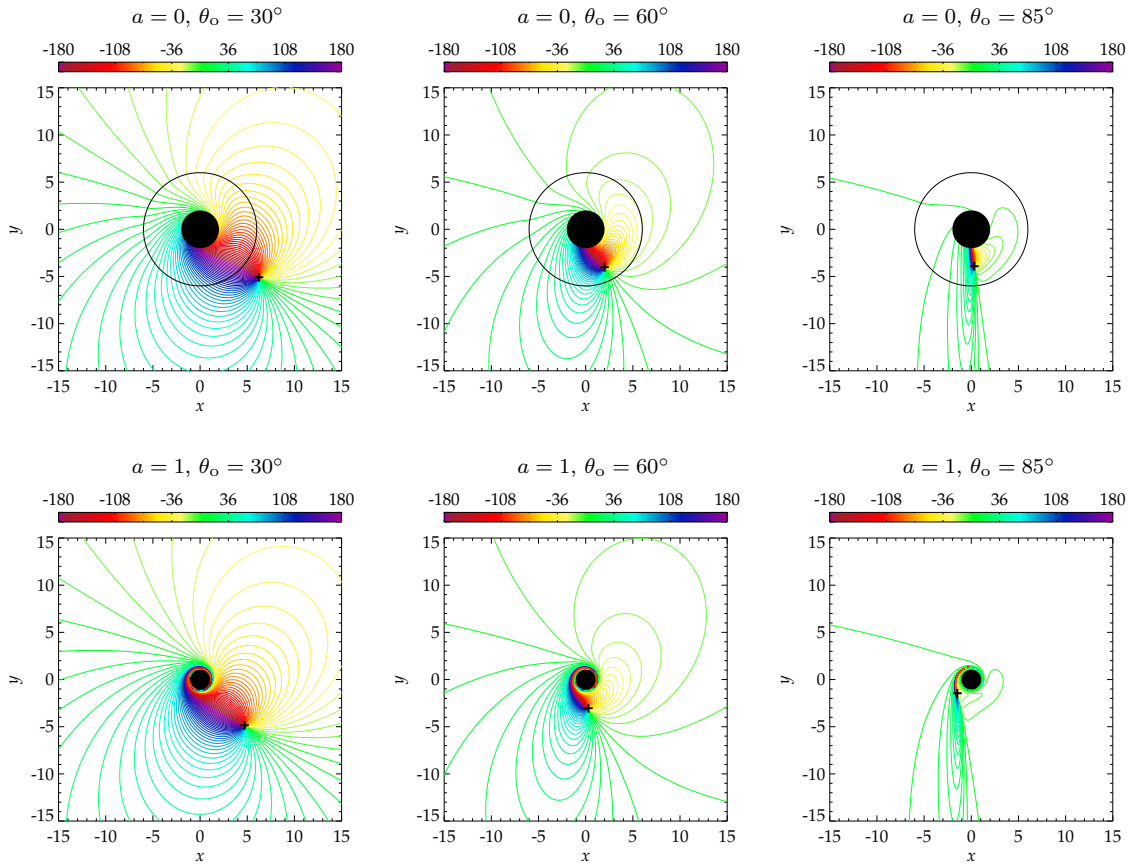

Figure 3. Contour graphs of the change of the polarization angle for Schwarzschild (top) and extreme Kerr (bottom) black hole. The observer inclination is $\theta_\mathrm{o} = 30°$, $60°$ and $85°$ (left to right). The observer is located to the top of the pictures. The innermost stable circular orbit is shown for the Schwarzschild case. The critical point, where the photons are emitted perpendicularly to the disc, is shown by a cross. The black hole rotates counter-clockwise in the Kerr case. The graphs are represented in the coordinates $x = r\cos\varphi$, $y = r\sin\varphi$ in the equatorial plane where r and φ are Boyer-Lindquist coordinates.

θ_o is the observer's inclination, κ_1 and κ_2 are components of the complex Penrose-Walker constant of parallel transport along geodesic κ_pw (Walker & Penrose 1970)

$$\kappa_1 = arp_\mathrm{e}^\theta f^t - r\,[a\,p_\mathrm{e}^t - (r^2+a^2)\,p_\mathrm{e}^\varphi]f^\theta - r(r^2+a^2)\,p_\mathrm{e}^\theta f^\varphi\,, \tag{12}$$

$$\kappa_2 = -r\,p_\mathrm{e}^r f^t + r\,[p_\mathrm{e}^t - a\,p_\mathrm{e}^\varphi]f^r + arp_\mathrm{e}^r f^\varphi\,. \tag{13}$$

Here, the polarization vector f^μ is

$$f^\mu = \frac{n^\mu - \mu_\mathrm{e}\,(g\,p_\mathrm{e}^\mu - U^\mu)}{\sqrt{1-\mu_\mathrm{e}^2}}\,. \tag{14}$$

with U^μ being the four-velocity of the co-rotating accretion disc[1]. Thus it is chosen to be in the direction of the x-axis in the above defined local frame on the disc.

[1] Below the innermost stable circular orbit we consider a free fall with the conserved energy and angular momentum of the matter on the marginally stable orbit. Note however, that we use this region only when computing the change of the polarization angle on Fig. 3. The thermal emission is neglected in this region.

4 POLARIZATION AT DETECTOR

The local polarization induced by scattering (see Fig. 1) is defined in the local frame co-moving with the disc. The intrinsic polarization angle is perpendicular to the disc axis for large optical depths and parallel for small optical depths. Photons are travelling in a curved space-time, which changes their polarization angle as seen at infinity, eq. (9), depending on the particular trajectory of each photon. This results in a depolarizing effect, when all photons will be eventually summed up at infinity, see eqs. (5)–(8).

Due to aberration the change of the polarization angle for each photon is different at infinity even in the Schwarzschild space-time (Pineault 1977). In the Kerr case the rotation of polarization vector because of the gravitational dragging is added. The dependence of the change of the polarization angle on the position of the emission from the disc is shown in Fig. 3. It can be seen that at large distances from the black hole this change is small. Therefore the depolarizing effect of the integration over this part of the disc will be also relatively small. On the other hand, below the critical point, where the light is emitted perpendicularly to the disc (see Fig. 3), the change of the polarization angle can acquire any value. Thus the depolarizing effect of this region is large. Therefore for the overall polarization mea-

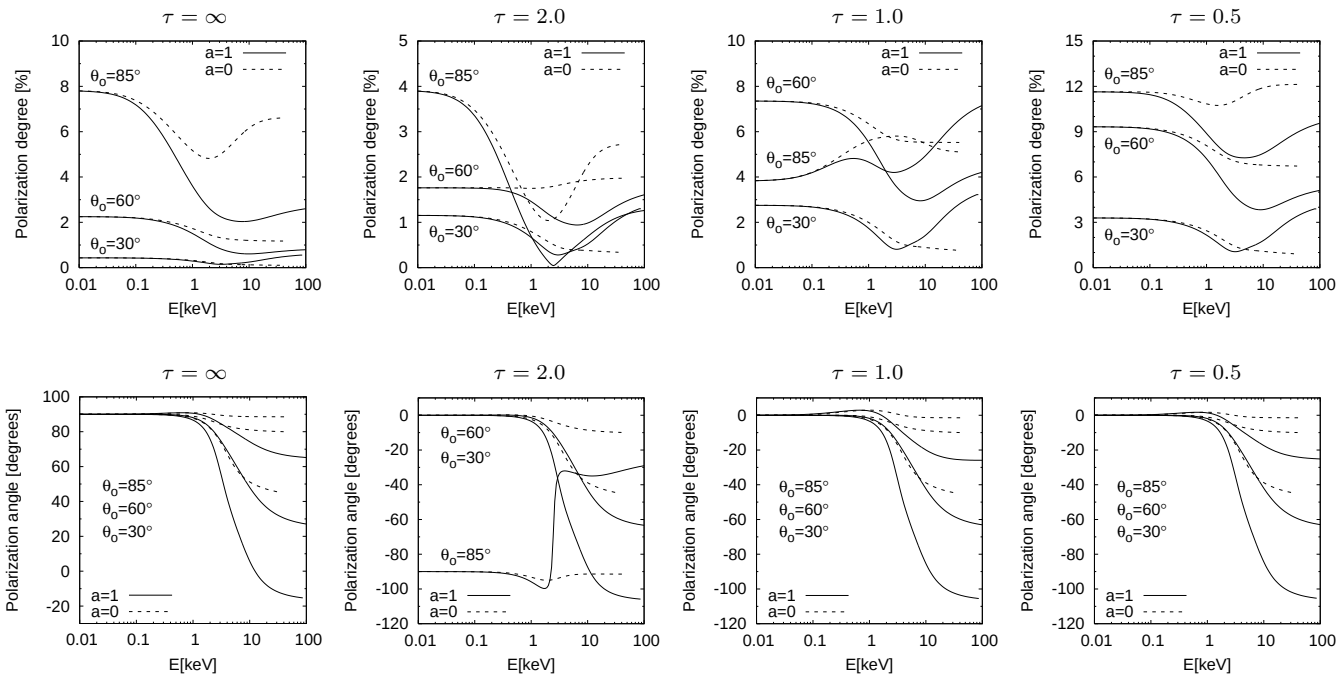

Figure 4. The energy dependence of the polarization degree (top) and polarization angle (bottom) as the observer at infinity would measure them for different optical depths of the atmosphere $\tau = \infty$, 2.0, 1.0, 0.5 (from left to right), in the case of the Schwarzschild (dashed lines) and extreme Kerr (solid lines) black holes and observer inclinations of 30°, 60° and 85°. A polarization angle of 0° represents the direction aligned with the projected symmetry axis of the disc.

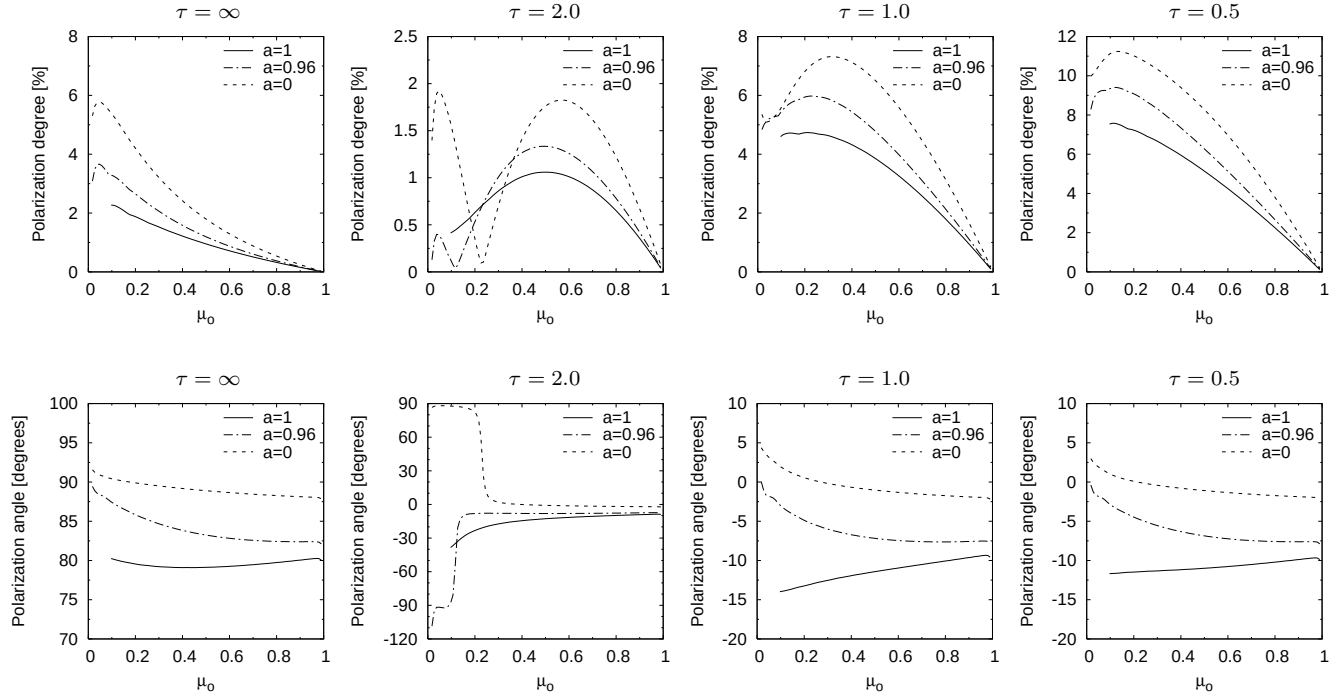

Figure 5. The dependence of the polarization degree (top) and polarization angle (bottom) at infinity on cosine of the observer's inclination for different optical depths of the atmosphere $\tau = \infty$, 2.0, 1.0, 0.5 (from left to right), in the case of the Schwarzschild (dashed lines) and extreme Kerr (solid lines) black holes. A polarization angle of 0° represents the direction aligned with the projected symmetry axis of the disc.

sured at infinity it is important if this critical point is above or below the marginally stable orbit.

It is clear that the depolarizing region is smaller for lower spin of the black hole. Note also that the area of the depolarizing region is larger for lower inclinations of the observer (the critical point moves farther away from the black hole).

The decrease of the temperature with the disc radius implies that, the closer to the black hole the radiation is emitted, the harder it is. As a consequence, the effects of GR are larger at higher energies. The energy dependence of the polarization degree and angle at infinity is shown in Fig. 4. In the low energy limit, i.e. for $E \lesssim 0.1$ keV, where the radiation is emitted far away from the black hole, the polarization degree and angle are basically equal to the local ones for the emission angle equal to the inclination of the observer (compare with the Fig. 1). In general, the polarization is highest for these energies because, as said above, GR effects tend to depolarize the radiation emitted from regions closer to the central black hole.

For high energies (above 10 keV), the polarization degree also increases. The polarization here is influenced mainly by that region of the disc, where the transfer function is the largest and the temperature is the highest. This area is not very large and thus the span of the change of the polarization angle is small. Therefore the depolarizing effect is not very large. Note, however, that for the same reason (small area) the flux for this interval of energy is also very small (see Fig. 2).

The dependence of the polarization degree and angle on the inclination of the observer is shown in Fig. 5. Both quantities are integrated over the whole energy range (0.01–100 keV). The polarization degree in most cases increases with the inclination angle of the observer. The polarization angle does not change much with the observer's inclination and optical depth, apart from the highest inclinations. Its value depends, quite strongly, on the spin of the black hole.

5 OBSERVATIONAL PERSPECTIVE

The development of X-ray polarimeters based on the photoelectric effect has renewed the interest in the polarimetry of X-ray astronomical sources. Until now, the only positive detection is that of the Crab Nebula (Weisskopf et al. 1978). The *Gas Pixel Detector* (GPD, Costa et al. 2001; Bellazzini et al. 2006a, 2007) is one of the most advanced project in this field. Its current design allows a large increase of performances with respect to the instruments built so far, with a sensitivity peaking at about 3 keV and a response between 2 and 10 keV.

The GPD has been proposed as a focal plane instrument, coupled with an X-ray optics, for several satellite missions. Here we discuss two feasible scenarios:

- a relatively small, low-cost pathfinder mission, possibly dedicated to the X-ray polarimetry, which could perform the study of Galactic and bright extragalactic sources. Long pointed observations are possible in this scenario and polarimetry at the level of ∼1% could be reached in a few days of observation, depending on the flux of the source;
- a large observatory, which could be dedicated to the study of the faint extragalactic sources and to the detailed investigation of the most interesting ones, following the results from the pathfinder missions. In this scenario, the lower time dedicated to the X-ray polarimetry will be balanced by the larger area of the optics.

We use two examples from the two scenarios above to verify if the effects presented in Sec. 4 will be measurable by the next missions with the GPD on-board. In the former profile, various missions are currently under study and hence there are concrete possibilities that at least one mission with an X-ray polarimeter based on the GPD will be launched in a few years. One of the options is POLARIX (Costa et al. 2006), an Italian mission dedicated to the X-ray polarimetry. Its design is now under Phase A study by the Italian Space Agency and, if eventually selected, POLARIX will be launched between 2012 and 2014. The baseline assumes three optics and even an improved version with six telescopes is considered. As a benchmark for the pathfinder missions, we considered this improved design of POLARIX, with the warning that, for the baseline version, the same results can be achieved by doubling the observing time.

With regard to the large mission scenario, the GPD was also inserted in the focal plane of the XEUS mission (Bellazzini et al. 2006b), which was proposed to ESA for the Cosmic Vision 2015-2025 and has passed the first selection step. It is now considered as a possible focal plane instrument for the International X-ray Observatory (IXO) mission, arising from the merging of the former XEUS and Constellation-X missions. Because the details of the IXO mission have not been fixed yet, we use the XEUS design (e.g. Arnaud et al. 2008) as benchmark for the large observatory scenario.

We choose the prominent Galactic black hole system and microquasar GRS 1915+105 to see how the next missions could investigate the GR effects on the degree and angle of polarization presented in Sec. 4. This source is very bright in the thermal state and the inclination of 70° (Mirabel & Rodriguez 1994) favours a high degree of polarization (see Fig. 4). We consider the spectrum in a low-luminosity thermal state (McClintock et al. 2006), $L \lesssim 0.3\,L_{\rm edd}$, to minimize contamination by a nonthermal component of emission. The dependence of the polarization with energy is that calculated in the Sec. 4 with $\tau = 1.0$ and $\theta_0 = 70°$. The presented results are computed for the hardening factor $f = 1.7$, mass of the black hole $M_\bullet = 14 M_\odot$ (Greiner, Cuby & McCaughrean 2001) and for the accretion rate $\dot{M} = 1.4 \times 10^{18}$ g/s (McClintock et al. 2006).

We assume the performances of the current prototype of the GPD simulated by means of a Monte Carlo software, which have been essentially confirmed by recent measurements (Muleri et al. 2008). The measured degree and angle of polarization are derived from convolving the response of the GPD with the expected degree of polarization and adding a Poisson background.

The results for the pathfinder scenario are shown in Fig. 6 for an observation of 500 ks, while those for a large mission are reported in Fig. 7 for an observation lasting 100 ks. The variation with energy is easily observed for both degree and angle of polarization. The Kerr and the Schwarzschild cases can be clearly discriminated (the errors shown are at the 3-σ level).

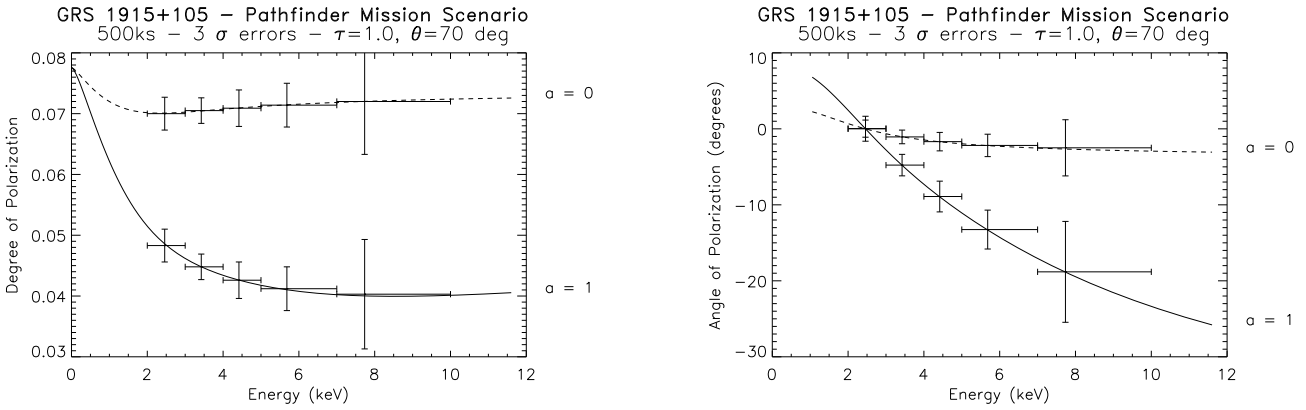

Figure 6. Energy dependence of the degree (left) and angle (right) of polarization, measured with an observation of 500 ks by the pathfinder mission. The solid and dashed curves refer to the case of a Kerr and Schwarzschild black hole respectively, with $\tau = 1.0$ and $\theta_0 = 70°$. Errors are quoted at the 3-σ level. Note that we set the angle of polarization to zero at low energy; the actual offset of the observed angle depends on the inclination of the accretion disk, which is unknown at this stage.

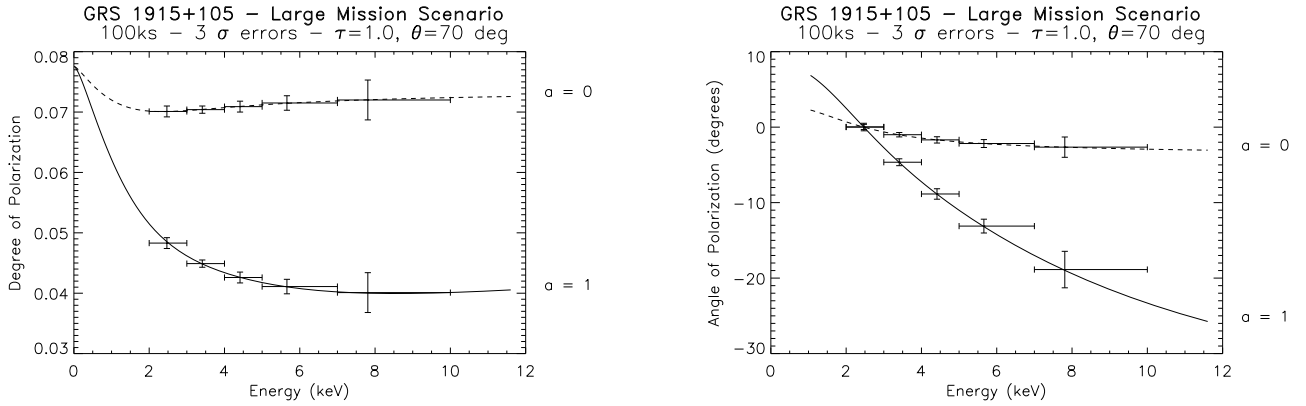

Figure 7. The same as the Fig. 6 but for the large mission scenario and an observation of 100 ks.

6 SUMMARY

We have investigated the GR effects on the polarization properties of the thermal radiation emitted by an accretion disc around a stellar mass black hole. The polarization at infinity is changed from its local value due to strong gravity effects and fast orbital motion of the disc close to the central black hole. The difference is particularly dramatic especially in the region below the critical point, where the polarization angle swings over the entire range of 180 degrees.

The most interesting interval of energy is from 0.1 to 10 keV. Below this energy band the emission comes from far away from the disc centre, while above this range the flux rapidly decreases. Note, however, that for different maximum temperatures of the disc the value of the upper boundary of this energy interval will change. All studied energy dependences will be shifted to a higher energy for a hotter disc. The maximum temperature is a function of the black hole mass, accretion rate and hardening factor as can be seen from the eq. (1).

The polarization degree is the highest for the lowest studied optical depth of the disc's atmosphere and in most cases it grows with the observer's inclination. The polarization angle does not change much with the inclination of the observer apart from the highest inclinations. Instead, it depends quite strongly on the spin of the central black hole.

The effects of strong gravity on the polarization state of emergent radiation will be accessible to the next missions with an X-ray polarimeter based on the Gas Pixel Detector. We presented the case of the pathfinder mission, feasible in a few years, and that of a large mission. In both scenarios, the energy dependence of the degree and of the angle of polarization will clearly discriminate between the Kerr and the Schwarzschild black holes cases. Even in the pathfinder scenario, the X-ray polarimetry will be a powerful probe of the metric around black holes.

ACKNOWLEDGMENTS

The authors acknowledge E. Costa, P. Soffitta and R. Bellazzini for making available the information on sensitivity of the GPD for the POLARIX and IXO missions.

This research is supported by the ESA Plan for Cooperating States project No. 98040 in the Czech Republic. MD and VK gratefully acknowledge support from the Czech Science Foundation grant 205/07/0052. RG is grateful for financial support to the Centre of Theoretical Astrophysics

(LC06014). FM and GM gratefully acknowledge the hospitality of the Astronomical Institute in Prague and, in particular, that of VK and MD. FM also acknowledges financial support from Agenzia Spaziale Italiana (ASI) under contract ASI I/088/06/0.

REFERENCES

Arnaud M. et al. 2008, Experimental Astronomy, in press
Bellazzini R. et al. 2006a, NIMA, 566, 552
Bellazzini R. et al. 2006b, Space Telescopes and Instrumentation II: Ultraviolet to Gamma Ray. Edited by Turner, Martin J. L.; Hasinger, Günther. Proceedings of the SPIE, Volume 6266, p. 62663Z
Bellazzini R. et al. 2007, NIMA, 579, 853
Beloborodov A. M. 1998, ApJL, 496, L105
Chandrasekhar S. 1960, Radiative Transfer (New York: Dover)
Connors P. A., Stark R. F. 1977, Nature, 269, 128
Connors P. A., Stark R. F., Piran T. 1980, ApJ, 235, 224
Costa E., Soffitta P., Bellazzini R., Brez A., Lumb N., Spandre G. 2001, Nature, 411, 662
Costa E. et al. 2006, Space Telescopes and Instrumentation II: Ultraviolet to Gamma Ray. Edited by Turner, Martin J. L.; Hasinger, Günther. Proceedings of the SPIE, Volume 6266, p. 62660R
Cunningham C. T. 1975, ApJ, 202, 788
Dovčiak, M. 2004, PhD thesis, arXiv:astro-ph/0411605
Dovčiak M., Karas V., Matt G. 2004a, MNRAS, 355, 1005
Dovčiak M., Karas V., Yaqoob T. 2004b, ApJSS, 153, 205
Dovčiak M., Karas V., Matt G., Yaqoob T. 2004c, in Proc. of Workshops on Black Holes and Neutron Stars, eds. S. Hledík and Z. Stuchlík (Opava: Silesian University), pp. 33–73
Goosmann R. W., Gaskell C. M. 2007, A&A, 465, 129
Greiner J., Cuby J.G., McCaughrean M.J. 2001, Nature, 414, 522
Laor A., Netzer H., Piran T. 1990, MNRAS, 242, 560
Liu J., McClintock J. E., Narayan R., Davis S. W., Orosz J. A. 2008, ApJ, 679, L37
Matt G. 1993, MNRAS, 260, 663
Matt G., Fabian A. C., Ross R. R. 1993, MNRAS, 264, 839
McClintock J. E., Shafee R., Narayan R., Remillard R. A., Davis S. W., Li L.-X., 2006, ApJ, 652, 518
Miller J. 2007 ARA&A, 45, 441
Mirabel I. F., Rodriguez L. F. 1994, Nature, 371, 46
Muleri F. et al. 2008, NIMA, 584, 149
Novikov I. D., Thorne K. S. 1973, in Black Holes, eds. C. DeWitt and B. S. DeWitt (New York: Gordon and Breach Publishers), p. 343
Page D. N., Thorne K. S. 1974, ApJ, 191, 499
Pineault S. 1977, MNRAS, 179, 691
Shakura N. I., Syunyaev R. A. 1973, A&A, 24, 337
Shimura T., Takahara F. 1995, ApJ, 445, 780
Silantev N. A., Gnedin Y. N. 2008, A&A, 481, 217
Stark R. F., Connors, P. A. 1977, Nature, 266, 429
Walker M., Penrose R., 1970, Commun. Math. Phys., 18, 265
Weisskopf M. C., Silver E. H., Kestenbaum H. L., Long K. S., Novick R. 1978, ApJ, 220, L117